PROCEEDINGS OF SCIENCE

Gamma-ray burst afterglows as probes of the ISM

P. Schady[*1], **S. Savaglio**[1], **T. Krühler**[2], **M.J. Page**[3], **J. Greiner**[1], **A. Rau**[1], **T. Dwelly**[1], **S.R. Oates**[3]

[1] *Max-Planck-Institut für Extraterrestrische Physik, Giessenbachstraße 1, 85748 Garching, Germany*

E-mail: pschady@mpe.mpg.de

[2] *The UCL Mullard Space Science Laboratory, Holmbury St Mary, Surrey, RH5 6NT, UK*

[3] *Dark Cosmology Centre, Niels Bohr Institute, University of Copenhagen, Juliane Maries Vej 30, 2100 Copenhagen, Denmark*

The immensely bright and intrinsically simple afterglow spectra of gamma-ray bursts (GRBs) have proven to be highly effective probes of the interstellar dust and gas in distant, star-forming galaxies. Despite significant progress, many aspects of the host galaxy attenuating material are still poorly understood. There is considerable discrepancy between the amount of X-ray and optical afterglow absorption, with the former typically an order of magnitude higher than that expected from the optical line absorption of neutral element species. Similar inconsistencies exist between the abundance of interstellar dust derived from spectroscopic and photometric data, and the relation between the line-of-sight and integrated host galaxy interstellar medium (ISM) remains unclear. In these proceedings we present our analysis on both spectroscopic and photometric multi-wavelength GRB afterglow data, and summarise some of the more recent results on the attenuation properties of the ISM within GRB host galaxies.

Gamma-Ray Bursts 2012 Conference -GRB2012,
May 07-11, 2012
Munich, Germany

[*] Speaker.

PoS(GRB 2012)062

1. Introduction

A causal connection between long gamma-ray bursts (GRBs) and massive star formation is now well established, and their immensely bright afterglows therefore pinpoint regions of distant star formation independent of galaxy luminosity. Moreover, due to their featureless, broadband afterglow, the imprint from attenuating material within the host galaxy can be studied in detail, providing a truly unique view of the interstellar medium (ISM) within distant star forming galaxies. Their incredibly bright and multi-wavelength afterglow not only illuminates the gas and dust within the star forming regions of the host galaxy, but also that of the interstellar material in the disk and halo of the galaxy, and intervening intergalactic medium along the GRB line-of-sight.

In these proceedings we summarise our work, as well as other published results on the various components of attenuating gas, metals and dust within the host galaxies of GRBs. Our analysis makes use of X-ray through to near-infrared (nIR) spectroscopic and photometric data, comprising one of the most complete studies on the attenuation properties of the ISM within GRB host galaxies. In particular, we address the nature of the excess X-ray absorption (section 2), and discuss the observed variation in the dust extinction properties of GRB host galaxies (section 3). In section 4 we summarise our results and provide some future prospects.

2. Afterglow absorption from intervening gas and metals

GRB afterglow spectra with coverage of the neutral hydrogen Lyman-α absorption feature (rest-frame 1215Å) show the clear presence of large column densities of cold ($T \leq 10^3$ K) neutral gas, $N_{\rm H}$, within the majority of GRB host galaxies. In many cases $N_{\rm H} > 10^{20.3}$ cm^{-2}, and the neutral absorbing gas component is thus referred to as a damped-Lyman-α (DLA) system, for which the ionisation correction is negligible. The survival of certain species, such as Mg I, and time varying Fe II and Ni II fine-structure lines, place this neutral gas component at a few hundred parsecs from the GRB (e.g. [1]), within the ISM of the host galaxy. The neutral ISM is also traced by low ionisation species detected in the ultraviolet (UV), whereas highly-ionised species (e.g. O IV, C IV, Si IV and N V) possibly probe the hot gas (T$\sim 10^4$ K) within the circumburst environment of the GRB [2], as well as a contribution from gas in the rest of the galaxy [3].

In contrast to the specific regions of gas that can be identified from UV spectra, X-ray spectroscopic observations provide measurements of the total column density of gas along the line-of-sight, probing both the cold neutral gas as well ionised regions. Soft X-rays with energies < 0.8 keV are absorbed by medium-weight metals along the line-of-sight, the most abundant of which is oxygen. Furthermore, the cross-section of oxygen is relatively insensitive to ionisation state [4]. The column of soft X-ray absorbing gas is thus a good proxy for the total oxygen column density along the GRB line-of-sight.

It is also the case that soft X-rays can be absorbed by metals locked in dust grains. Such absorption at UV and optical wavelengths would not be detected, since at these wavelengths light is instead scattered by dust grains, resulting in the smooth attenuation of the UV/optical GRB afterglow (see section 3). Nevertheless, most GRB lines-of-sight are fairly dust-poor, with $\sim 50\%$ having a visual dust extinction, A_V, consistent with zero [5]. The contribution to soft X-ray absorption from metals condensed onto dust is therefore usually small.

There is now known to be a considerable discrepancy between X-ray and optical afterglow absorption measurements, whereby the equivalent neutral hydrogen column density derived from soft X-ray absorption (assuming solar abundances), $N_{\rm H,X}$, is typically an order of magnitude higher than the neutral hydrogen column density $N_{\rm H}$ derived from Lyman-α absorption [6]. One possibility is that this is produced by a significant column of ionised gas that is transparent to UV photons [6]. To explore this option further, we re-analysed the optical and X-ray absorption in GRB afterglows, but used absorption lines of singly-ionised metals rather than Lyman-α to trace the neutral gas within GRB host galaxies [7]. Such analysis enables a direct comparison between the optical and soft X-ray absorption features, since both are produced by metals. Furthermore, by removing the need for Lyman-α absorption and host galaxy metallicity measurements, the latter being frequently uncertain or unavailable, the sample size of GRBs with the necessary data increases. We took a sample of 26 GRBs with detected optical spectroscopic absorption lines in at least one of Zn II, Si II, S II or Fe II, and with available X-ray afterglow spectroscopic data.

2.1 Total versus neutral gas

To trace the neutral gas within a GRB host galaxy, we used either Zn II, S II, Si II or Fe II, with the most refractive, and thus least preferential species listed last. When only Si II or Fe II absorption measurements were available, a dust correction was applied to the measured column density. We then corrected for cosmic abundance variances by normalising all our measurements to each other using the abundances from [8]. We denote the normalised column densities of oxygen (measured from soft X-ray absorption), zinc, silicon, sulphur and iron (all measured from UV absorption lines) by $N_{N,O}$, $N_{N,Zn}$, $N_{N,Si}$, $N_{N,S}$ and $N_{N,Fe}$, respectively.

In the left panel of Fig. 1 we show the neutral gas column density, $N_{\rm ntr}$, against $N_{\rm N,O}$, which represents the total column of gas (neutral and partially ionised). $N_{\rm ntr}$ corresponds to either $N_{\rm N,Zn}$ (red circles), $N_{\rm N,S}$ (orange squares), $N_{\rm N,Si}$ (green stars) or $N_{\rm N,Fe}$ (blue triangles), where both $N_{\rm N,Si}$ and $N_{\rm N,Fe}$ have been corrected for dust depletion. The dashed line in Fig. 1 (left panel) corresponds to where the column density of neutral gas is equal to the total column density of gas as probed by our X-ray absorption measurements. From this figure it is clear that for all GRBs, $N_{\rm N,O}$ is larger than the column density of neutral gas, $N_{\rm ntr}$, by around an order of magnitude, implying that over 90% of the gas along the line-of-sight is ionised.

There is an indication that the difference between the soft X-ray and neutral metal absorption increases for smaller column densities. This would suggest that the fraction of ionised gas is not dependent on the global galaxy properties, but on local conditions, such as would be the case if the GRB itself were the dominant source of ionising photons. Nevertheless, this trend is not significant, and we can thus only speculative at this stage.

2.2 Highly ionised gas

To explore further the ionisation state of the X-ray absorbing gas we looked into the contribution from highly ionised gas, which, unlike neutral gas, can be found within the circumburst environment of the GRB [2, 3]. We used a sample of nine GRBs with absorption from highly ionised species (i.e., C IV, Si IV, N V and O VI) detected in the optical afterglow spectrum [2, 3, 9]. To quantify the contribution to soft X-ray absorption from highly ionised gas, we normalised the soft

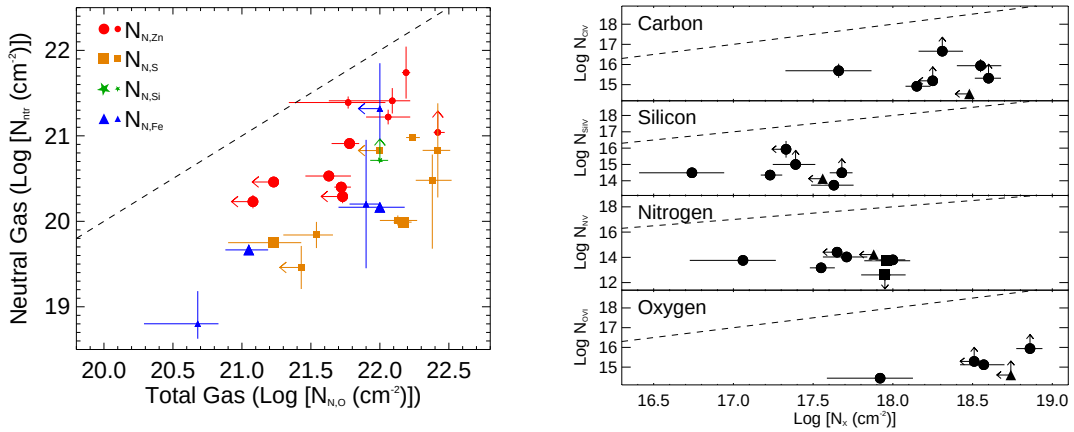

Figure 1: ***Left:*** Host galaxy neutral gas column density, $N_{\rm ntr}$, against host galaxy total gas column density, $N_{\rm N,O}$, along the line-of-sight to a sample of 26 GRBs. For each GRB, $N_{\rm ntr}$ is derived from either the column density of Zn II (red circles), S II (orange squares), Si II (green stars) or Fe II (blue triangles), where a correction for dust depletion is applied to $N_{\rm N,Si}$ and $N_{\rm N,Fe}$. Smaller data points correspond to those taken from low- or mid-resolution spectra, and larger data points are taken from high-resolution spectra (R $> 10,000$). The dashed line corresponds to where $N_{\rm ntr}$ is equal to $N_{\rm N,O}$. ***Right:*** Logarithmic host galaxy column density of the highly ionised atoms C IV, Si IV, N V and O VI against the total logarithmic column densities of C, Si, N and O in the top, second, third and bottom panels, respectively. The total column densities are derived from X-ray observations, denoted by N_X. The C IV, Si IV, N V and O VI measurements plotted as circles are all taken from [3], the N V data plotted as squares are from [2], and data taken from [9] are plotted as triangles. In all four panels, the dashed line corresponds to where the normalised soft X-ray column density is equal to the column density of the corresponding highly ionised atom.

X-ray absorption measurements to the cosmic abundance of the element used to trace the highly ionised gas (i.e. either Si, C, N or O). Our results are shown in Fig. 1 (right panel), which compares the logarithmic column density of the highly ionised atoms N_{CIV}, N_{SIV}, N_{NV} and N_{OVI} against the soft X-ray absorption column densities normalised to C, Si, N and O cosmic abundances in the top, second, third and bottom panel, respectively. The latter is denoted by N_X, where X corresponds, from top-most panel, to the respective element C, Si, N or O. In all four panels the dashed line is where the normalised soft X-ray column density is equal to the column density of the highly ionised atom indicated on the y-axis.

It is clear from this figure that all data points lie several orders of magnitude below the dashed lines, indicating that the highly ionised gas within GRB hosts only makes up a small fraction ($< 0.01\%$) of the soft X-ray absorption. The left-hand panel in Fig. 1, on the other hand, indicates that $\sim 90\%$ of the gas probed by the soft X-rays is ionised. If the large fraction of this gas is in a lower ionisation state, then there should be a signature of this in the detection of strong absorption lines from intermediate ionisation lines with ionising potentials (IPs) between ~ 20 eV and ~ 50 eV (i.e. Si II and Si IV). This is, however, not the case. For example, Al III, which has an IP of 28 eV, is frequently observed to be weaker than Al II, which has an IP of 19 eV. This would, therefore, suggest that most of the ionised gas probed by the soft X-rays is in an ultra-ionised state, with IPs larger than ~ 200 eV. The signature left by such an ultra-ionised gas would lie predominantly in the soft X-ray energy range, which is already heavily absorbed by oxygen and carbon (both neutral and ionised). Resolving the absorption from an ultra-ionised gas is, therefore, beyond the spectral

capabilities of current fast-response X-ray telescopes.

Other suggested explanations for the soft X-ray excess absorption have been an underestimate of the absorption from metals within the Milky Way, absorption from intervening systems [10], or absorption within the local Universe from a diffuse 'warm-hot' intergalactic medium, or WHIM [11].

3. Afterglow dust extinction

Another source of attenuation is in the absorption and scattering of light, or *extinction*, caused by intervening dust. The amount of dust extinction along a single line-of-sight is, for the most part, an inverse function of wavelength. This dependence on wavelength is known as the *dust extinction curve*, and it is a function of both the grain size distribution and composition of the extinguishing dust. Extinction curves therefore vary with environment, and this seen within the local Universe, in the average extinction curve observed within the Milky Way, and the Large and Small Magellanic Clouds (LMC and SMC respectively) (see Fig. 2). The greatest differences between these extinction curves is in the prominence of an extinction feature centred at $\sim$ 2175Å (most pronounced along Milky Way sight lines, negligible within the SMC), and in the slope of the curve at UV and optical wavelengths, which is flattest within the Milky Way, and steepest within the SMC.

The UV/optical power-law GRB afterglow spectrum allows the broad, smooth shape cut-out by dust-extinction to be measured with relative ease, making GRBs ideal probes to the extinction properties of dust beyond the local Universe. Model-fits to the broadband spectral energy distribution (SED) of GRB afterglows with different template extinction curves (predominantly Milky Way, SMC and LMC) typically yield best-fit results when using an SMC-like dust extinction curve and visual extinction $A_V < 0.3$ (e.g. [12, 13, 14]). Although for a given SED, the best-fit A_V will increase the flatter that the template extinction curve used is, the above results are based mostly on GRBs with sensitive, nIR to X-ray afterglow coverage, for which the shape of the extinction curve is well-constrained. These results are thus robust. There is, however, an extended tail in the A_V distribution, with $\sim$ 10% of GRB sight lines showing host galaxy extinction $A_V > 1$ [5], many of which also have much flatter, Milky Way-like host extinction curves than observed in the hosts of only moderately extinguished GRBs. The large measured visual extinction of $A_V > 1$ does not change significantly with the host extinction curve fitted, and the observed relation between size of A_V and flatteness of extinction curve is thus not an artefact of the fitting procedure. There are now four GRBs with spectroscopically confirmed detections of a 2175Å absorption bump at the redshift of the GRB host galaxy [15], as well as several GRBs with a 2175Å extinction feature detected in the GRB SED. The causes for this range in A_V and in the shape of the extinction curves of GRB hosts, and how the dust properties along the GRB line-of-sight relate to the GRB host galaxy global properties are still poorly understood.

3.1 Heavily dust-extinguished GRB sightlines

Around 40% of GRBs have their optical afterglow suppressed by either neutral gas within the intergalactic medium, or more commonly, from dust within the host galaxy [5, 19]. For these so-called 'dark' GRBs, the arcsecond position provided by the optical afterglow is therefore not avail-

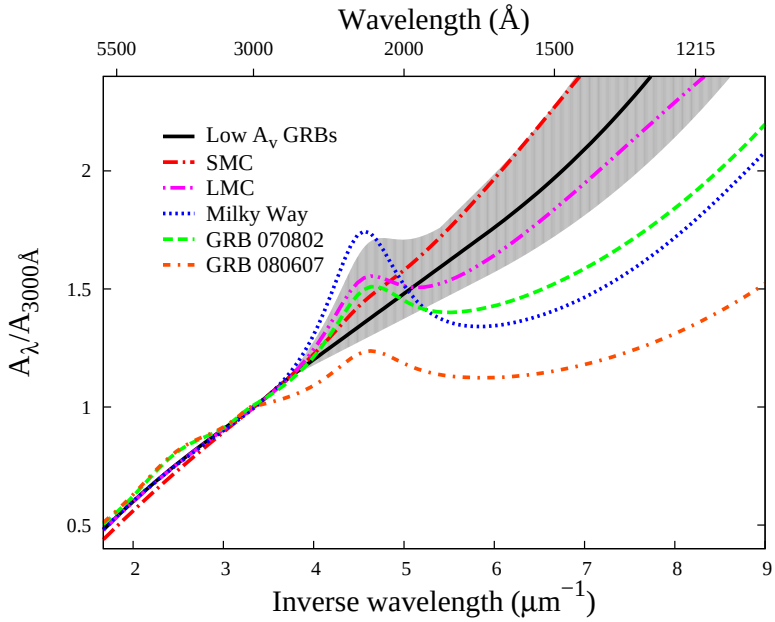

Figure 2: Best-fit mean GRB host extinction law as derived from simultaneous SED fits normalised at A_{3000} (black) and corresponding 90% confidence region (grey) [14]. Also shown for comparison are the mean SMC (red, dot-dash), LMC (pink, dot-dot-dash) and Milky Way (blue, dotted) extinction laws [16], as well as the best-fit extinction curves to the two heavily extinguished GRBs, GRB 070802 (green, dashed; [17]) and GRB 080607 (orange, dot-dot-dashed; [18]).

able, introducing a clear bias against follow-up observations of their host galaxies. The improved positional accuracy of GRBs provided by the rapid response of *Swift* and (semi-)robotic ground-based telecopes, in particular those equipped with nIR instruments, has significantly improved our ability over the last half decade to study highly dust-extinguished GRBs and their host galaxies. A leading instrument in acquiring broadband observations that extend into the nIR wavelength range has been the GRB optical and nIR detector (GROND; [20]), commissioned in July 2007. GROND is unique in providing simultaneous $g'r'i'z'$ and nIR JHK observations of the early-time afterglow, and has proved highly effective at detecting and measuring host galaxy dust extinction for a large sample of GRBs [5], and increasing the host galaxy visual extinction distribution out to $A_V > 1$. Other nIR instruments such as PAIRITEL[1] have also greatly contributed.

This reduction in the selection effects against dusty lines-of-sight has also seen an increase in the variety of GRB host galaxy properties. Most optically-selected host galaxies, which make up the majority of the population, are young, star-forming, low-mass galaxies [21, 22], with sub-solar metallicities. Recent follow-up observations of the host galaxies of heavily extinguished GRBs have, nevertheless, indicated the environmental conditions traced by GRBs to be much more diverse than indicated by previous, optically biased observations.

3.1.1 Dependence of extinction curves on A_V and on global galaxy properties

There is empirical evidence that the prominence of the 2175Å extinction bump and the overall flatness of the extinction curve is related to the total visual extinction, A_V, along the line-of-sight. The few GRB host extinction curves with a spectroscopically detected 2175Å extinction bump

[1] http://www.pairitel.org/

also correspond to GRB lines-of-sight with some of the largest visual extinctions. There is some evidence that the host galaxies of highly dust-extinguished GRBs are typically more massive, luminous, and chemically evolved than the typical host galaxies of relatively unextinguished GRBs (e.g. [23]). Nevertheless, despite such observed trends, the relation between the GRB line-of-sight, and the global host galaxy properties remains far from clear.

One of the most dust-extinguished GRBs (GRB 080607; [18]) also had one of the flattest extinction curves and most prominent 2175Å bumps detected along a GRB line-of-sight. Its very red host galaxy ($R-K>5$; [24]) indicated the dust to be ubiquitous within the galaxy, and it had a stellar mass $M_{*}\sim 8\times10^{9}\ M_{\odot}$; almost an order of magnitude larger than the hosts of unextinguished GRBs ($\langle M_{*}\rangle\sim10^{9}\ M_{\odot}$; [22]). On the other hand, GRB 070306 and GRB 100621A were two other heavily extinguished GRBs ($A_V\sim5.5$ and $A_V\sim3.8$ respectively), but both with very blue host galaxies, with $R-K$ colours comparable to the host galaxies of relatively unextinguished GRBs [23], indicative of a very clumpy distribution of dust. Furthermore, although GRB 070306 had one of the largest stellar masses measured for a long GRB host galaxy ($2\times10^{10}\ M_{\odot}$; [23]), the host stellar mass for GRB 100621 ($10^{9}\ M_{\odot}$) was comparable to that of optically bright afterglow host galaxies.

3.1.2 Dust-to-metals ratio

The visual extinction-to-metals column density ratio, $A_V/N_{\rm H,X}$, within GRB host galaxies along the GRB line-of-sight has been investigated in a number of papers, and these ratios have typically been found to be much higher than the ones observed in the Local Group (e.g. [13, 25, 26, 27, 28]). The large majority of these studies have, nevertheless, been biased towards unextinguished lines-of-sight, and recent samples of GRBs with $A_V>4$ have shown metals-to-dust ratios significantly below the previous average, and more in line with observations along lines-of-sight within the Local Group [23]. This inverse trend between the metals-to-dust ratio and A_V along GRB lines-of-sight suggests that the absorbing metals are associated with the host-galaxy rather than with intervening systems. Such an inverse relation may be expected if two physically independent absorbers lie along the line-of-sight: a dust-free, ionized plasma in the GRB circumburst environment, and another dusty and more distant, thus less ionised cloud [23]. Such a model is supported by the observed dependency between GRB host galaxy dust-to-gas ratios and ISM metallicity, which is consistent with that observed in the local Universe, and indicates that the exinguishing dust is related to the host galaxy neutral gas component [15].

4. Summary and future prospects

The move towards combining both imaging and spectroscopic data from across the spectrum, and ongoing programmes dedicated at pushing down observational biases in GRB afterglow and host galaxy samples, are providing a more rounded view on the local and global environments of GRBs, and on the effect that the GRB explosion has on the circumburst material.

The large UV radiation field implied by $\sim90\%$ of the gas within GRB hosts being in an ultra-ionised state has implications for the effect of massive star formation on the surrounding environment. Direct detection of an ultra-ionised gas component requires early-time, high spectral-

resolution X-ray data, which is currently unattainable. Nevertheless, a useful verification would be to model the UV radiation field and circumburst properties required to satisfy observations.

Finally, the tantalising evidence that GRBs may reside in more varied environmental conditions than previously speculated (i.e., with no metallicity cap), would suggest that GRBs make better tracers of the cosmic star formation rate density than had previously been thought, and certainly places GRBs as truly unique probes of the dust properties and ionisation state of the ISM within high-z, star-forming galaxies. How the attenuation along the GRB sight line relates to the global host galaxy properties is not yet clear, and this requires further investigation through dedicated, broadband (including nIR) afterglow follow-up campaigns to acquire a larger sample of *unbiased*, and thus more representative GRB afterglow and host galaxy observations.

References

[1] Vreeswijk et al. 2007, *A&A*, 468, 83

[2] Prochaska, J. X., et al. 2008, *ApJ*, 685, 344

[3] Fox et al. 2008, *A&A*, 491, 189

[4] Verner, D. A., & Yakovlev, D. G. 1995,*A&AS*, 109, 124

[5] Greiner, J., et al. 2011, *A& A*, 526, A30

[6] Watson, D., et al. 2007, *ApJ*, 660, 101

[7] Schady, P., et al. 2011, *A&A*, 525, 113

[8] Asplund, M., et al. 2009, *AEA&A*, 47, 481

[9] D'Elia, V., et al. 2010, *A&A*, 523, 36

[10] Campana, S., et al. 2012, *MNRAS*, 421, 169

[11] Behar, E.., et al. 2011, *ApJ*, 734, 26

[12] Kann, D. A., Klose, S., & Zeh, A. 2006, *ApJ*, 641, 993

[13] Schady, P., et al. 2010, *MNRAS*, 401, 2773

[14] Schady, P., et al. 2012, *A&A*, 537, 15

[15] Zafar, D., et al. 2011, *A&A*, 532, 143

[16] Pei, Y. C. 1992, *ApJ*, 395, 130

[17] Elíasdóttir, Á., et al. 2009, *ApJ*, 697, 1725

[18] Perley, D. A., et al. 2011, *AJ*, 141, 36

[19] Perley, D. A., et al. 2009, *AJ*, 138, 1690

[20] Greiner, J., Bornemann, W., Clemens, C., et al. 2008, PASP, 120, 405

[21] Le Floc'h, et al. 2003, A&A, 400, 499

[22] Savaglio, S., Glazebrook, K., & Le Borgne, D. 2009, *ApJ*, 691, 182

[23] Krühler, T., et al. 2011, *A& A*, 534, 108

[24] Chen, H.-W., et al. 2011, *ApJ*, 727, L53

[25] Galama, T. J., & Wijers, R. A. M. J. 2001, *ApJ*, 549, L209

[26] Stratta, G., Fiore, F., Antonelli, L. A., Piro, L., & De Pasquale, M. 2004, *ApJ*, 608, 846

[27] Starling, R. L. C., et al. 2007, *ApJ*, 661, 787

[28] Schady, P., et al. 2007, *MNRAS*, 377, 273